

Existence of Colloidal Primitive Building Units Exhibiting Memory Effects in Zeolite Growth Compositions

V. Radha Rani, Ramsharan Singh, Pramatha Payra, and Prabir K. Dutta*

Department of Chemistry, 120 West 18th Avenue, The Ohio State University, Columbus, Ohio 43210

Received: July 14, 2004; In Final Form: October 11, 2004

This study focuses on the clear, stable mother liquors obtained after completion of crystallization of nanocrystalline sodalite, zeolite A, and zeolite Y. Characterization of the freeze-dried mother liquors by high-resolution transmission electron microscopy showed regions of crystallinity for both zeolites A and Y, and ~5 nm regions of crystallinity could be identified in zeolite Y. Upon adding the mother liquor to nutrient solutions of aluminates and silicates, it was found that the mother liquor could direct formation of the corresponding framework, thereby manifesting a memory effect. Dynamic light scattering studies showed that there were units present in the mother liquors that grew into crystals at a faster rate than the parent compositions used to generate the mother liquors. We propose that the mother liquors recovered after crystallization contain primary structural units having memory of the zeolite formed and that these units can assemble to form viable nuclei if provided with a source of nutrients.

1. Introduction

The nucleation and growth of aluminosilicate zeolites and related microporous materials continues to be an area of active research.¹ Even with modern spectroscopic and analytical measurements, the complexity of the synthesis process has eluded a molecular level understanding. The early events that lead to nucleation and subsequent zeolite growth are not well understood, especially the molecular features that direct a particular composition to a specific framework. For systems that involve transformation of a gel to crystalline phase, the problem is even more difficult. Nevertheless, advances have been made in understanding the synthesis process as well as development of new framework structures.

In particular, synthesis of zeolites from “clear” solutions,^{2–4} i.e., from solutions that do not lead to a gel, has made it possible to monitor the crystallization process by various physical techniques. Examples include ²⁹Si MAS NMR,^{6,7} dynamic light scattering,^{5,8} ultra-small-angle X-ray scattering (USAXS), and wide-angle X-ray scattering (WAXS).^{9,10} Such studies have detected nanometer-sized precursors in the synthesis solutions, and aggregation of these units to eventually form crystals has been proposed. Most detailed studies have been reported on the silicalite-1 system.^{11–13} Schoeman first reported the presence of 2.8 nm particles in a silicalite composition based on cryotransmission electron microscopy, light scattering, and chemical methods.^{3,13} A more precise structural model proposed formation of nanoslabs via combination of specific “trimer” silicate species and their subsequent aggregation to form crystals.¹⁴ However, this mechanism has come under criticism since other NMR studies have not found the large, open-framework silicate species.^{15,16} More recently, transmission electron microscopy studies have also provided insight into the controversy.^{17,18} High-resolution electron microscopic studies have noticed the evolution of amorphous nanometer-sized amorphous particles of 40–80 nm to crystals of zeolite A and 25–35 nm particles to zeolite Y.^{19,20} AFM studies of the (111)

face of zeolite Y has revealed triangular terraces 1.5 nm in height, corresponding to the width of a faujasite sheet.²¹ Terraces were proposed to nucleate and grow in a layer-by-layer fashion on clean surfaces and therefore the necessity of high levels of supersaturation. On zeolite A surface, step heights of 1.2 nm, which corresponds to one-half unit cell in the (100) direction, was observed, and the crystal growth was proposed to occur with much higher rates at kink sites.²¹

The role of aged reactant compositions in shortening the induction period is well-known.¹⁰ In addition, addition of aged aluminosilicate solutions prior to synthesis as well as seed crystals is known to speed up crystallization, primarily by acting as a nuclei source, thereby shortening the induction period.^{1,8} The nature of zeolitic nuclei and how they are formed is of great interest. We address this issue by investigating the properties of solutions that were recovered after zeolite crystallization was complete. Trying to study nucleation by examining solutions after crystal growth is complete may sound counterintuitive, but the motivation to approach the study in this manner is because of the numerous studies that suggest the presence of nanometer-sized units throughout the crystallization process.^{3,14,19}

In this study, we focus on nanocrystalline sodalite, zeolite A, and zeolite Y synthesized from clear solutions. Typically, the yields of zeolites from such compositions are quite low.^{2–4} Our interest is in the clear, stable mother liquors obtained after completion of the crystallization of the nanocrystalline zeolites. The question we pose is the following: do these mother liquors have a memory of the zeolites? To demonstrate the manifestation of the memory effect, we have examined if solutions recovered from different zeolite syntheses can direct nutrient solutions to the corresponding framework. The dynamics of crystal growth was carried out using dynamic light scattering studies. Characterization of the freeze-dried solutions recovered from the crystallization was carried out with high-resolution transmission electron microscopy. From these data, we have been able to draw conclusions about the zeolite nucleation process.

* To whom correspondence should be addressed. E-mail: dutta.1@osu.edu.

TABLE 1: Composition for Synthesis of Nanocrystalline Zeolites (NC)²²

zeolite	(TMA) ₂ O	Na ₂ O	Al ₂ O ₃	SiO ₂	H ₂ O	time (days)	yield (%)
SOD	14	0.85	1	40	805	2	3.5
LTA	14	0.85	4	40	805	1.25	30
FAU	5.07	0.65	1.62	7	805	3	1.6

TABLE 2: Results of Crystallization Experiments with Mother Liquor and Various Compositions

ML	NC	time (days)	phase obtained	yield (g)
Composition A:				
15.19(TMA) ₂ O:0.63Na ₂ O:1.6Al ₂ O ₃ :44.9SiO ₂ :805H ₂ O at 98 °C				
SOD		3	SOD	0.4157
LTA		3	LTA	0.0569
FAU		3	no product	
	SOD	3	no product	
	LTA	3	no product	
	FAU	3	no product	
Composition B:				
13.68(TMA) ₂ O:~0.05Na ₂ O:2.188Al ₂ O ₃ :~9.34SiO ₂ :805H ₂ O at 98 °C				
FAU		1	FAU, LTA (minor)	0.1335
	FAU	1	amorphous	
Composition C:				
~6.48(TMA) ₂ O:~0.05Na ₂ O:2.188Al ₂ O ₃ :~9.34SiO ₂ :805H ₂ O at 98 °C				
FAU		1	FAU	0.2514
	FAU	1	amorphous	

2. Experimental Section

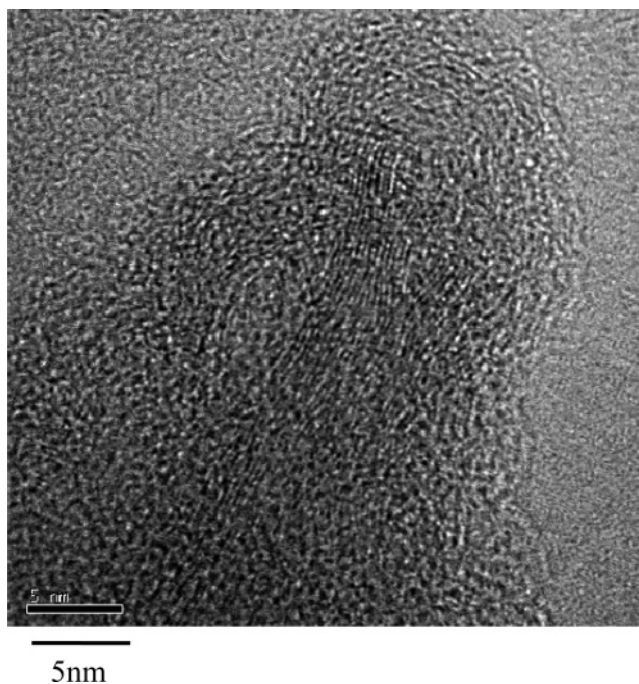
2.1. Materials. The reagents used for preparing the synthesis solution were Ludox SM-30 colloidal (30 wt % suspension in water) from Aldrich, tetramethylammonium hydroxide (25 wt % aqueous solution) from Sachem, Inc., aluminum hydroxide (80.5%) from Alfa Aesar, and distilled water. Other materials used in this work were sodium hydroxide from Mallinckrodt and DOWEX HCR-S ion-exchange resin (20–50 dry mesh) from Aldrich for pH adjustment.

2.2. Synthesis Procedure for Zeolites Y and A and Sodalite from Clear Solutions. The synthesis of zeolites A and Y and sodalite from a clear aqueous solution with a molar composition²² as given in Table 1 were performed at 98 °C. Tetramethylammonium hydroxide was added to an aqueous solution of aluminum hydroxide and stirred to give a clear solution. Then slowly silica sol was added with constant vigorous stirring, and the resulting solution was further stirred for about 30 min. For carrying out the crystallization, the solutions in Teflon bottles were transferred to a 98 °C preheated oil bath. All samples were centrifuged using a high-speed ultracentrifuge at 24 000 rpm to remove the solid material, which was then washed and dried in a vacuum oven at 60 °C. The mother liquor, left behind after centrifugation, was used for further studies.

2.3. Characterization. The solid samples were characterized by X-ray diffraction (XRD). The XRD data were collected on a Rigaku Geigeflex X-ray diffractometer using Cu K α radiation. The scanning electron microscopic (SEM) pictures of these samples were collected using a JEOL JSM-820 SEM instrument.

2.4. Synthesis Experiments with Mother Liquors. The synthesis experiments were carried out by adding 10 vol % of the mother liquor to different compositions shown in Table 2. There was no visible cloudiness upon mixing these solutions, and they were transferred to a 98 °C preheated oil bath for crystallization. The products obtained after ultracentrifugation were examined by capillary XRD.

2.5. Dynamics of Nuclei Growth. The growth of particles in various compositions was monitored using dynamic light scattering. The analyses were performed with an argon ion laser (Coherent Innova 90C), with a wavelength of 514.5 nm.

**Figure 1.** High-resolution TEM of freeze-dried SOD(ML).

Scattered light was monitored by a photomultiplier tube set at 90° to the incident beam. The samples to be measured were filtered through a 0.2 μ m pore diameter directly into clean glass scattering cells. The scattering cell with the reaction mixture was placed in a thermostated holder (at 98 °C), and the data were acquired at short intervals during which the particle growth occurred. The method of cumulants was used for data analysis.

2.6. Isolation of the Nuclei. The mother liquors obtained from the three nuclei solutions were freeze-dried using LAB-CONCO Freezone 12. The crystallinity in the freeze-dried samples was identified by high-angle annular dark field scanning transmission electron microscopy (STEM) using an FEI Tecnai F20 TEM/ STEM. The samples were prepared by depositing a drop of an ultrasonicated methanol suspension on a carbon-coated Cu grid. The grid was dried at room temperature and mounted on a specimen holder. Micrographs were recorded at 200 kV.

3. Results

3.1. Choice of Zeolite Systems. The zeolite systems that were the focus of this study were nanocrystalline sodalite, zeolite A, and zeolite Y. The nanocrystalline synthesis compositions (NC) were derived from the patent literature and are shown in Table 1.²² Crystallization of the frameworks was confirmed by X-ray powder diffraction, and electron microscopic studies of the products show crystals of ~50, ~100, and ~50 nm for sodalite, LTA, and zeolite Y, respectively. These results are consistent with literature.^{3,22} Mother liquors (MLs) were recovered after ultracentrifuging the nanocrystals. These MLs were optically clear for over 6 months and are henceforth labeled as SOD-(ML), LTA(ML), and FAU(ML), for sodalite, zeolite A, and zeolite Y, respectively. The goal of this study was to examine how these ML solutions from the nanocrystalline syntheses manifest memory of the crystals.

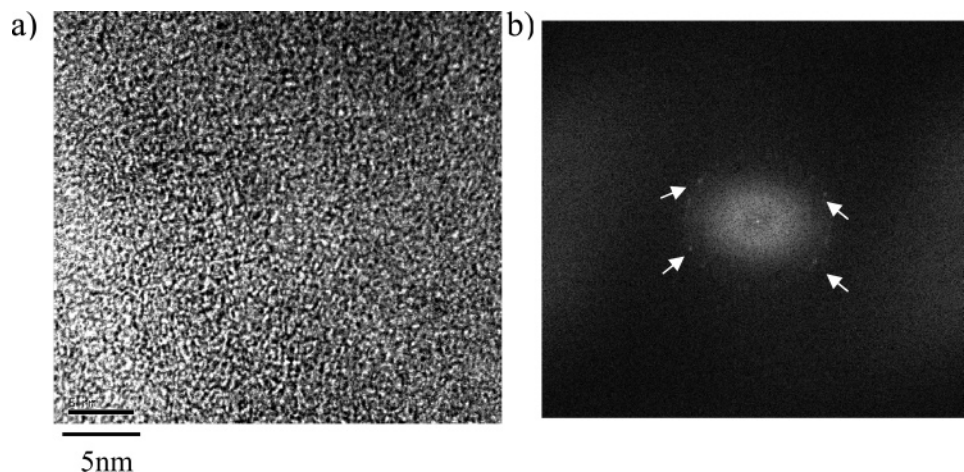


Figure 2. High-resolution TEM from freeze-dried LTA(ML). (a) TEM of a region that exhibited crystallinity; (b) electron diffraction pattern from crystalline region.

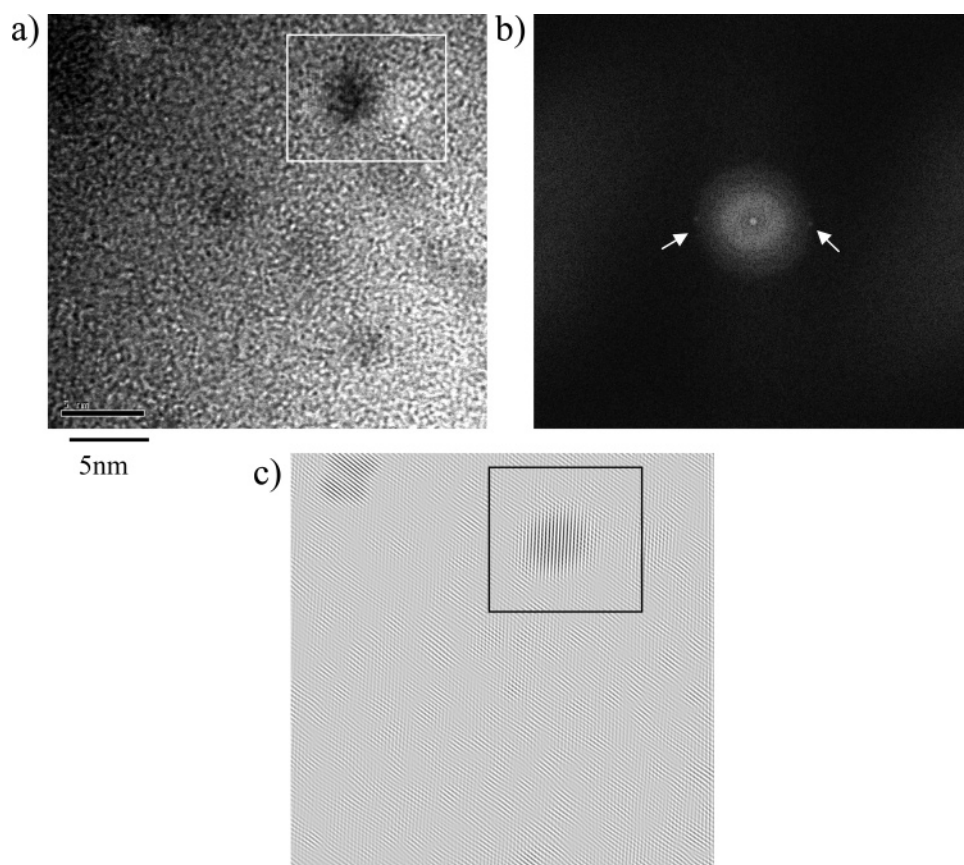


Figure 3. High-resolution TEM of freeze-dried FAU(ML). (a) STEM of region that exhibited crystallinity; (b) electron diffraction from boxed region of (a); (c) inverse Fourier transform image of (a).

3.2. Characterization of the Particles Present in ML

Dynamic light scattering studies showed the presence of particles of sizes ~ 30 , 73, and 193 nm for SOD(ML), LTA(ML), and FAU(ML), respectively, at room temperature, which upon heating to 98 °C decreased to 11, 8, and 23.1 nm, respectively. The decrease in particle size upon heating is possibly from the deagglomeration of the particles formed upon cooling the ML solutions. To examine the nature of the particles present, the ML solutions were freeze-dried and examined by high-angle annular dark field STEM. The strategy in the electron microscopy experiments was to survey the electron diffraction pattern of the sample under view, followed by obtaining micrographs of regions that showed evidence of crystallinity. With the lyophilized SOD(ML), an extensive search led to no appearance

of crystallinity. There were some regions where the solid appeared “ordered”, as shown in Figure 1, but no diffraction patterns were observed. For LTA(ML), regions with crystallinity were observed, an example of which is shown in Figure 2a. A typical electron diffraction pattern from this region is shown in Figure 2b. Weak spots indicating a crystalline region is evident; however, these were very susceptible to beam damage, and the diffraction patterns would disappear quickly in the presence of the stationary electron beam. The freeze-dried solutions derived from FAU(ML) synthesis showed the most direct example of isolated crystalline regions, and the data are shown in Figure 3. The regions marked on the figure showed diffraction patterns indicative of crystallinity (Figure 3b). To enhance the contrast, an inverse Fourier transformation was performed and the image

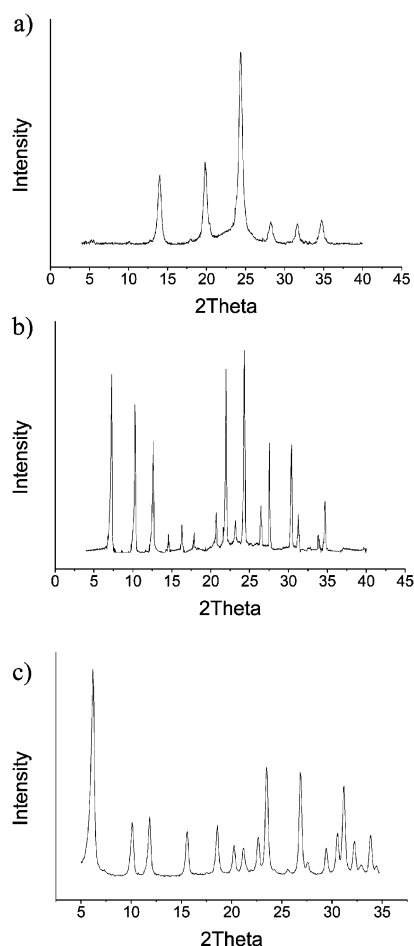


Figure 4. Powder diffraction patterns of zeolites grown from mixing of ML and compositions shown in Table 2. (a) SOD(ML) with composition A; (b) LTA(ML) with composition A; (c) FAU(ML) with composition C.

is shown in Figure 3c. These crystalline regions were on the order of ~ 5 nm and susceptible to beam damage.

3.3. Synthesis Experiments with ML. To examine how the ML solutions manifest memory of the crystals that the solutions originated from, a series of experiments were carried out. The strategy was as follows. The goal was to find nutrient compositions (containing aluminate and silicate) to which if unheated NC solutions (Table 1) were added and then heated to 98°C , there was no appearance of crystals in a certain period of time. Then, with the same nutrient composition, the experiment was repeated with the addition of the corresponding ML, and the formation of crystals within the same period was examined. For example, consider nutrient composition A shown in Table 2. To this composition we added the unheated, parent solutions (NC) from Table 1. The volume ratios were 9 parts composition A and 1 part NC composition, chosen so as not to perturb composition A. As shown in Table 2, addition of NC led to no product formation after 3 days of heating. Then, the identical experiment with composition A was repeated, but instead of adding the parent NC solution, the corresponding ML that was recovered after the crystallization process was added. After 3 days, SOD(ML) led to the formation of sodalite, LTA(ML) led to the formation of zeolite A, and FAU(ML) did not lead to the formation of any product. Two other compositions B and C shown in Table 2 were examined with FAU(NC) and FAU(ML). For both these compositions, the addition of the NC led to an amorphous material after 1 day of heating, whereas with FAU(ML) zeolite Y was obtained. With compositions B and

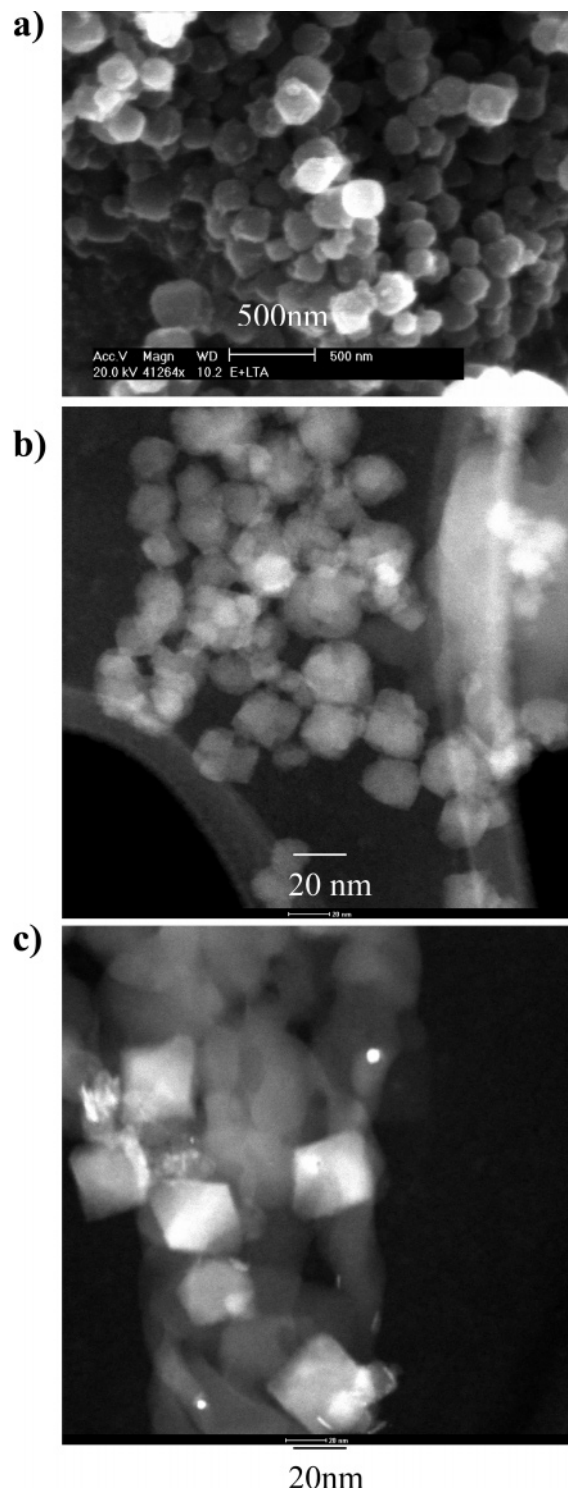


Figure 5. (a) Scanning electron micrograph of zeolite A; (b) TEM of sodalite; (c) TEM of zeolite Y (all grown by mixing of ML and compositions A and C).

C, addition of NC solutions for sodalite and LTA led to formation of mixtures of zeolites Y and LTA and, therefore, the effects of SOD(ML) and LTA(ML) could not be evaluated. Figures 4 and 5 show the XRD and SEM of sodalite, zeolite A, and zeolite Y recovered from the ML addition experiments (composition C for FAU) in Table 2. From the diffraction patterns, it is obvious that pure frameworks are being formed in all cases. From the electron microscopy data, the sizes of the zeolite particles mirror the same trend as obtained from the NC compositions, with zeolite A being on the order of 200 nm whereas sodalite and zeolite Y are on the order of 25 nm.

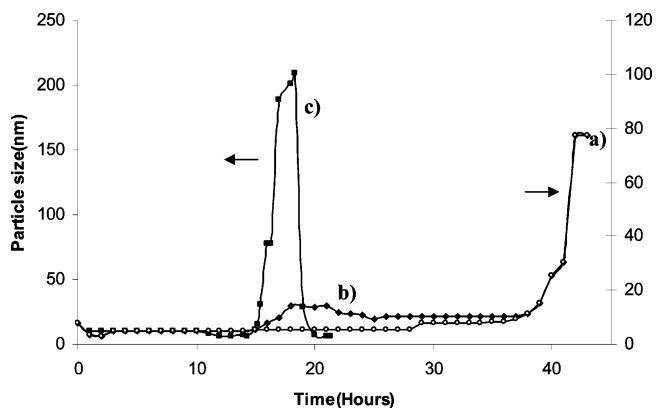


Figure 6. Dynamic light scattering studies at 98 °C of solutions of (a) SOD(NC) (○), (b) SOD(ML) added to SOD(NC) (◆), and (c) SOD(ML) with composition A (■).

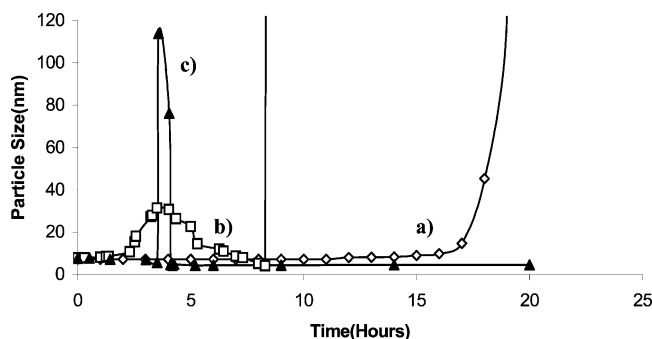


Figure 7. Dynamic light scattering studies at 98 °C of solutions of (a) LTA(NC) (◇), (b) LTA(ML) added to LTA(NC) (□), and (c) LTA(ML) with composition A (▲).

3.4. Dynamics of Growth. Dynamic light scattering studies were carried out at 98 °C, primarily focusing on the sodalite and zeolite A system and the compositions shown in Tables 1 and 2. Figure 6 shows the comparison of three sets of growth experiments for sodalite. Figure 6a is the growth of sodalite with the SOD(NC) composition, Figure 6b is SOD(ML) added to SOD(NC), and Figure 6c is the growth of SOD(ML) added to composition A. For the SOD(NC) composition, particle sizes remain below 10 nm until about 40 h, when crystal growth is observed. For SOD(ML) added to composition A, particles remain at 11 nm until 16 h followed by rapid growth, reaching a maximum of 209 nm at 20 h. There is a decrease in particle size at longer times that arises from agglomeration of the particles and settling. For SOD(ML) added to SOD(NC) two particle growth processes were observed, one peaking around 20 h, followed by the second growth at 40 h (overlapping with the SOD(NC) growth).

Figure 7 shows the light scattering data for zeolite A, with LTA(NC) and LTA(ML) added to composition A and LTA(NC). Several features of these growth studies are comparable to the sodalite system, with the addition of LTA(ML) introducing an earlier crystal growth event (~4 h) when added to either NC or composition A. The difference is that addition of SOD(ML) does not alter the regular growth kinetics of NC composition, but LTA(ML) did speed up the process with a very large growth spurt at 8 h. All light scattering experiments were repeated at least twice.

4. Discussion

There are many reports in the literature on using zeolites as seed crystals.¹ In particular, a study where a particular composition led to different zeolites depending on the seed crystal added

is of interest.²³ The composition $90\text{Na}_2\text{O}:9\text{SiO}_2:1\text{Al}_2\text{O}_3:5760\text{H}_2\text{O}$ formed a clear solution from which zeolite Y emerged after 7 h at 80 °C. Addition of zeolite A seed crystals to this composition led to formation of zeolite A. Numerous other studies have shown that seed crystals can provide nuclei as well as provide surface sites for heterogeneous nucleation and growth.^{24,25} Our focus here is different: after nucleation is complete and crystallization is complete, does the remaining solution still have species that maintain a memory of the framework? If the answer is in the affirmative, and depending on how the memory effect is manifested, nucleation mechanisms can be developed. The basis for our hypothesis stems from the research of several investigators over the past decade. Schoeman reported the presence of ~2.8 nm particles during silicalite synthesis and proposed that these particles can grow to larger size or that structural features on their surface may act as nuclei.^{3,13} de Moor et al. confirmed the presence of ~2.8 nm particles in silicalite synthesis and proposed that these are primary building units which do assemble to form nuclei and then crystals.⁹ Most importantly, they speculated that the primary building units are distinct for each zeolite framework, but had enough order on a submicrometer scale to form nanometer-sized nuclei. We reasoned that if the primary building units are present after crystal growth, then solutions containing these units should exhibit a memory effect.

Our study focuses on three zeolite systems, sodalite, zeolite A, and zeolite Y. There were several reasons for choosing these three frameworks. First, the yields of nanocrystalline zeolites from the typical compositions are quite low, indicating that significant amounts of reactants are left behind in solution.²² Second, midsynthesis addition of reactants to these compositions leads to secondary nucleation, indicating that primary building units may be present.^{2,26}

Our synthesis experiments involved addition of small amounts of mother liquor from which crystal growth had occurred to different compositions, with an intention not to alter the ratio of various components in these compositions, but enabling it to direct these compositions to the specific zeolite. The data shown in Table 2 clearly demonstrate that the solutions recovered from synthesis of nanocrystalline zeolites are manifesting a memory effect. Composition A can be directed to sodalite or zeolite A, depending on the corresponding ML added. However, with FAU(ML), composition A did not lead to zeolite Y, whereas compositions B and C did. These results suggest that, for the species in ML to manifest the memory effect, the nutrient composition is also important.

Based on the dynamic light scattering studies of ML added to composition NC, two growth processes were observed for both sodalite and zeolite A. For the sodalite system, the growth process at longer times is what is expected for sodalite growth with the composition SOD(NC), with particle sizes stabilizing around ~37 nm and an induction time of ~40 h.² The earlier growth spurt is arising due to addition of SOD(ML) and takes about 20 h for crystal growth, immaterial of using composition A or SOD(NC). This would indicate that there are primary building units in the ML that grow into crystals. Since it takes ~20 h to grow into viable nuclei (as compared to 40 h), then the units present in ML must have some preformed structures associated with the crystal framework. For zeolite A, the presence of LTA(ML) leads to an earlier growth spurt at 4 h, again indicating the presence of building units that can form viable nuclei. In the case of zeolite A, LTA(ML) also must contain nuclei, which speeds up the latter growth spurt from 17 h to about 8 h.

One of the most detailed models about crystal growth was proposed on the basis of scattering studies on a silicalite composition and involved nucleation of the zeolite in two steps.⁹ First, there was the formation of 2.8 nm primary particles followed by aggregation to form 5–10 nm clusters, a fraction of which evolved to form viable nuclei. The primary particles contain five-membered silicate rings and could provide growth units to seed crystals, even under conditions where no nucleation took place. The present study offers support to this model. In the initial stages of the crystal growth, we observe ~10 nm particles. Electron microscopic results show that at least for LTA(ML) and FAU(ML) there are regions of crystallinity in the amorphous matrix, and for the FAU(ML) these can be identified as ~5 nm crystallites. Thus, the ~10 nm particles must be partly amorphous. We propose the hypothesis that the memory effects demonstrated by ML are occurring due to the ordered regions, and allude to these as the primary building units. Electron microscopic studies of clear synthesis solutions for zeolites A and Y have also noted the presence of amorphous gel particles, and with time the appearance of discrete crystalline regions in the gel particle.^{19,20}

We can subdivide the induction period into two parts: a prenucleation time to form the primary particles, which would be on the order of 20 h for sodalite (4 h for zeolite A), followed by another period over which the primary particles evolve to nuclei, which was another 20 h for sodalite (13 h for zeolite A). Because the ML already had the primary particles, an earlier growth spurt was observed. It is also clear that ML does not contain completely formed nuclei, since that would predict immediate growth upon providing a source of nutrients, and this is not the case. The question then arises as to why these primary units in ML did not continue to grow into viable nuclei in the original NC compositions. This is possibly related to limitation of reagents and supported by the midsynthesis reagent addition experiments that resulted in new crystal growth.^{2,26}

It is also then implied that the primary units in ML do not evolve into nuclei by just restructuring within the unit, but involve growth, as suggested for silicalite from scattering studies⁹ and for zeolites A and Y from electron microscopic studies. Another observation that supports the hypothesis related to limitation of reagents is that, for synthesis of nanocrystalline zeolite Y, the nucleation and crystal growth periods overlapped.²⁶

Moreover, as noted with the FAU(ML) added to composition A, the primary units only develop into nuclei in certain compositions. It is unclear if this is due to the instability of the primary unit in certain compositions, or if the evolution of the primary unit into nuclei is being compromised. de Moor et al. noted that in the case of silicalite, the 2.8 nm particles would only aggregate for forming viable nuclei if the alkalinity of the composition was within a certain range.⁹

Finally, the observations here can be contrasted with crystal growth of faujasitic microporous zincophosphates from reverse micelles, where the mother liquor was found to contain well-formed nuclei that grew immediately upon addition of nutrients.²⁷

5. Conclusions

There are several conclusions that can be drawn from this study. First, it appears that the synthesis compositions contain primitive structures that retain a memory of the zeolite framework even after crystallization is complete. These structures are possibly nanometer-sized particles (<5 nm) observed

in TEM and are embedded in larger amorphous particles seen by light scattering. Second, these units will manifest their memory if provided with the appropriate nutrients. Third, these units need to evolve into nuclei possibly by growing larger before their effect can be manifested. Fourth, the evolution of the primary building units into nuclei only occurs in certain reaction compositions, indicating, as has been noted in earlier papers, that the process of nuclei formation requires a specific type of interaction between the building units, and, therefore, is sensitive to composition. Thus, this study shows that, during nanocrystalline zeolite synthesis, there are specific primary particles present throughout the crystalline process that can grow to viable nuclei if provided with nutrients.

Acknowledgment. We acknowledge funding from NASA and helpful discussions with Dr. Brain Schoeman.

References and Notes

- (1) Auerbach, S. M.; Carrado, K. A.; Dutta, P. K. *Handbook of Zeolite Science and Technology*; Marcel Dekker: New York, 2003.
- (2) Schoeman, B. J.; Sterte, J.; Otterstedt, J. E. *Zeolites* **1994**, *14*, 208–216.
- (3) Persson, A. E.; Schoeman, B. J.; Sterte, J.; Otterstedt, J.-E. *Zeolites* **1995**, *15*, 611–619.
- (4) Schoeman, B. J.; Sterte, J.; Otterstedt, J. E. *Zeolites* **1994**, *14*, 110–116.
- (5) Schoeman, B. J.; Sterte, J.; Otterstedt, J. E. *J. Porous Mater.* **1995**, *1*, 185–198.
- (6) Ravishankar, R.; Kirschhock, C. E. A.; Knops-Gerrits, P. P.; Feijen, E. J. P.; Grobet, P. J.; Vanoppen, P.; De Schryver, F. C.; Mieh, G.; Fuess, H.; Schoeman, B. J.; Jacobs, P. A.; Martens, J. A. *J. Phys. Chem. B* **1999**, *103*, 4960–4964.
- (7) Houssin, C. J. Y.; Kirschhock, C. E. A.; Magusin, P. C. M. M.; Mojet, B. L.; Grobet, P. J.; Jacobs, P. A.; Martens, J. A.; Van Santen, R. A. *Phys. Chem. Chem. Phys.* **2003**, *5*, 3518–3524.
- (8) Gora, L.; Streletsky, K.; Thompson, R. W.; Phillis, G. D. *J. Zeolites* **1997**, *19*, 98–106.
- (9) de Moor, P. P. E. A.; Beelen, T. P. M.; Komanshek, Beck, L. W.; Wagner, P.; Davis, M. E.; Van Santen, R. A. *Chem. Eur. J.* **1999**, *5*, 2083–2088.
- (10) Singh, P. S.; Dowling, T. L.; Watson, N. J.; White, J. W. *Phys. Chem. Chem. Phys.* **1999**, *1*, 4125–4130.
- (11) Houssin, C. J. Y.; Mojet, B. L.; Kirschhock, C. E. A.; Buschmann, V.; Jacobs, P. A.; Martens, J. A.; Van Santen, R. A. *Stud. Surf. Sci. Catal.* **2001**, *135*.
- (12) de Moor, P. P. E. A.; Beelen, T. P. M.; Komanshek, B. U.; Diat, O.; Van Santen, R. A. *J. Phys. Chem. B* **1997**, *101*, 11077–11086.
- (13) Schoeman, B. J. *Zeolites* **1997**, *18*, 97–105.
- (14) Kirschhock, C. E. A.; Ravishankar, R.; Van Looveren, L.; Jacobs, P. A.; Martens, J. A. *J. Phys. Chem. B* **1999**, *103*, 4972–4978.
- (15) Knight, C. T. G.; Kinrade, S. D. *J. Phys. Chem. B* **2002**, *106*, 3329–3332.
- (16) Kragten, D. D.; Fedeyko, J. M.; Sawant, K. R.; Rimer, J. D.; Vlachos, D. G.; Lobo, R. F.; Tsapatsis, M. *J. Phys. Chem. B* **2003**, *107*, 10006–10016.
- (17) Ramanan, H.; Kokkoli, E.; Tsapatsis, M. *Angew. Chem., Int. Ed.* **2004**, *43*, 4558–4561.
- (18) Kirschhock, C. E. A.; Liang, D.; Aerts, A.; Aerts, C. A.; Kremer, S. P. B.; Jacobs, P. A.; Van Tendeloo, G.; Martens, J. A. *Angew. Chem., Int. Ed.* **2004**, *43*, 4562–4564.
- (19) Mintova, S.; Olson, N. H.; Valtchev, V.; Bein, T. *Science* **1999**, *283* (5404), 958–960.
- (20) Mintova, S.; Olson, N. H.; Bein, T. *Angew. Chem., Int. Ed.* **1999**, *38* (21), 3201–3204.
- (21) Anderson, M. W.; Agger, J. R.; Hanif, N.; Terasaki, O.; Ohsuna, T. *Solid State Sci.* **2001**, *3*, 809–819.
- (22) Otterstedt, J.-E.; Sterte, J.; Schoeman, B. J. PCT/SE93/00715, 1993.
- (23) Kumakiri, I.; Sasaki, Y.; Shimidzu, W.; Yamaguchi, T.; Nakao, S. *Stud. Surf. Sci. Catal.* **2001**, *135*.
- (24) Gora, L.; Streletsky, K.; Thompson, R. W.; Phillis, G. D. *J. Zeolites* **1997**, *18*, 119–131.
- (25) Subotic, B.; Bronic, J. In *Handbook of Zeolite Science and Technology*; Auerbach, S., Carrado, K. A., Dutta, P. K., Eds.; Marcel Dekker: New York, 2003; pp 129–204.
- (26) Li, Q.; Creaser, D.; Sterte, J. *Chem. Mater.* **2002**, *14*, 1319–1324.
- (27) Singh, R.; Dutta, P. K. *Langmuir* **2000**, *16*, 4148–4153.